Eurasian Journal of Physics and Functional Materials

Volume 8 | Number 3

Article 5

Pages: 131 - 147

2024

Exploration on the efficacy of Ag and CuO nanofluids for pouch lithium-ion batteries and its thermal management

Anitha Dhanasekaran
Faculty of Integrated Technologies, Universiti Brunei Darussalam, Gadong BE1410, Brunei,
anithadhanasekaran60@gmail.com

Yathavan Subramanian
Faculty of Integrated Technologies, Universiti Brunei Darussalam, Gadong BE1410, Brunei

Rajkumar Dhanasekaran
Department of Science & Humanities, University College of Engineering (Anna University), Arni, India

Ramesh Kumar Gubendiran
Department of Science & Humanities, University College of Engineering (Anna University), Arni, India

Abaniwo Rose Mafo
Department of Biochemistry, Prince Abubakar Audu University, Ayingba, Kogi State, Nigeria

See next page for additional authors

Recommended Citation

Dhanasekaran, Anitha; Subramanian, Yathavan; Dhanasekaran, Rajkumar; Gubendiran, Ramesh Kumar; Mafo, Abaniwo Rose; Raj, Veena; Yassin, Hayati; and Azad, Abul K (2024) "Exploration on the efficacy of Ag and CuO nanofluids for pouch lithium-ion batteries and its thermal management," *Eurasian Journal of Physics and Functional Materials*: Vol. 8: No. 3, Article 5.
DOI: https://doi.org/10.69912/2616-8537.1228

Exploration on the efficacy of Ag and CuO nanofluids for pouch lithium-ion batteries and its thermal management

Authors

Anitha Dhanasekaran, Yathavan Subramanian, Rajkumar Dhanasekaran, Ramesh Kumar Gubendiran, Abaniwo Rose Mafo, Veena Raj, Hayati Yassin, and Abul K Azad

ORIGINAL STUDY

Exploration on the Efficacy of Ag and CuO Nanofluids for Pouch Lithium-ion Batteries and its Thermal Management

Anitha Dhanasekaran [a,*], Yathavan Subramanian [a], Rajkumar Dhanasekaran [b], Ramesh K. Gubendiran [b,***], Abaniwo R. Mafo [c], Veena Raj [a], Hayati Yassin [a], Abul K. Azad [a,**]

[a] Faculty of Integrated Technologies, Universiti Brunei Darussalam, Gadong, BE1410, Brunei
[b] Department of Science & Humanities, University College of Engineering (Anna University), Arni, India
[c] Department of Biochemistry, Prince Abubakar Audu University, Ayingba, Kogi State, Nigeria

Abstract

Lithium-ion batteries still remain a cornerstone for the sustainable transportation by the way of its usage in electric vehicles (EVs). However, their optimal performance hinges on maintaining at consistent thermal conditions especially during operation, and at high discharge rates. The present study proposes a novel mini-channel cooling system specifically designed for a 10 Ah lithium-ion pouch cell. This innovative design incorporates cold plates on both battery surfaces for enhanced heat dissipation. In addition, the efficacy of silver (Ag) and copper oxide (CuO) nanofluid coolants by comparing with traditional water cooling in three distinct battery design configurations was also studied. Design 1 and 2 comprises respectively with partially and fully encased cold plates with mini-channels distributed both segmentally and centrally, and Design 3 the present proposed model featuring a fully covered cold plate with a serpentine flow layout for optimized heat transfer efficiency. Extensive computational analysis using ANSYS FLUENT 18.1 software reveals the superiority of Design 3. Notably, this configuration achieved significantly a lower maximum cell temperature (306.7 K and 305.0 K) with 0.25% and 0.5% Ag nanofluid coolants compared to Design 1 and 2, at a discharge rate of 5C. This underscores the potential of silver nanofluids for superior battery thermal management, particularly within the optimized Design 3 framework. These findings offer valuable insights for developing enhanced battery thermal management systems in EVs.

Keywords: Mini-channels, Nanofluids, Thermal management, Lithium-ion batteries, Electric vehicles

1. Introduction

In the domain of energy storage and environmental preservation, lithium-ion batteries (LIBs) are progressively supplanting traditional fuels and establishing themselves as the industrial norm [1—3]. Their growing popularity can be ascribed to their superior energy density, minimal self-discharge rates and extended lifespan. In 2021, global shipments of lithium-ion batteries reached a substantial production of 294.5 GWh, with China contributing significantly with 158.5 GWh [4]. This suggests an anticipated marginal increase in LIB demand over the next five years, as these batteries play a crucial role in new energy vehicles (NEVs) like EVs and hybrid EVs. Among the various types of LIBs, large-sized pouch-type batteries (PTB) emerge as the primary power source for NEVs due to their promising characteristics [5,6]. Specifically, the efficiency and safety of LIBs are intricately tied to their operational temperature and the temperature differentials among cells [7,8]. During charging and discharging cycles, significant heat is generated due to Joule's law of heating effect and entropy changes, resulting in a faster temperature rise. It is recommended [9] to maintain the

Received 19 August 2024; revised 8 September 2024; accepted 11 September 2024.
Available online 19 October 2024

* Corresponding author.
** Corresponding author.
*** Corresponding author.
E-mail addresses: anithadhanasekaran60@gmail.com (A. Dhanasekaran), rameshvandhai@gmail.com (R.K. Gubendiran), abul.azad@ubd.edu.bn (A.K. Azad).

https://doi.org/10.69912/2616-8537.1228

operating temperature of LIBs within a narrow range of 15~35 °C, with a permissible temperature difference of less than 5 °C among cells in a battery pack; otherwise, thermal runaway may occur, leading to battery explosion.

In view of above reasons, effective thermal management (TM) techniques are indispensable for these large-sized LIBs to address the substantial temperature rises and non-uniform temperature gradients. Numerous research efforts have been made to develop more promising battery thermal management systems (BTMS) and they are broadly categorized into various types. These fundamental BTM systems include air [10,11], liquid [12,13] and phase-change material cooling [14,15]. Both active & forced air and as well as liquid cooling systems (LCS) are currently in use for commercial EVs. As battery capacity and operating power increase, LCS are becoming the favorable choice due to their enhanced cooling performance and thermal conductivity [16]. Particularly, the design of flow channels plays a crucial role in the indirect-contact mode of liquid cooling. For cylindrical batteries, flexible structures like flat, wavy tubes etc., are typically employed, whereas cold plates with internal mini-channels are commonly used for energy dense PTB. In recent days, there has been significant interest in mini-channel liquid cooling systems. For instance, Huo et al. [17] devised a cold plate with parallel straight channels on the battery surface to analyze the cooling performance. Notably, Jia et al. [18] investigated the BTM using a traditional water-cooling approach on a 20 Ah $LiFePO_4$ Li-ion cell with a partially covered cold plate and mini-channels distributed segmentally and centrally. These insightful research findings have significantly influenced the design of mini-channel liquid cooling systems, offering valuable perspectives on the impact of diverse design and operating parameters. Relying on Jia et al.'s [18] design, Wu et al. [19] conducted valuable research to improve the model by employing a water-cooling approach through fully encased cold plates with mini-channels distributed both segmentally and centrally. Their proposed model exhibited superior cooling performance compared to Jia et al.'s [18] work and this serves as the foundation for this proposed research.

Even though Wu et al. [19] design has demonstrated good performance, it can be further improved by adopting innovative minichannel arrangements within cold plates. For instance, Jin et al. [20] designed a novel cold plate with oblique channels on the battery surface and compared it traditional (straight) channel configuration. Deng et al. [21] investigated a practical liquid cooling approach used for rectangular LIBs. The applied cooling system was a serpentine-channel-shaped cold plate to improve the cooling performance. Jarrett and Kim et al. [22] have developed a liquid cooling system incorporating a serpentine channel design. Computational Fluid Dynamics (CFD) simulations was utilized therein to refine the model focusing on optimizing parameters, such as the weighted average pressure drop and mean temperature. Based on this literature review, it is evident that adopting innovative cooling channel arrangements such as serpentine flow patterns within cold plates leads to better cooling performance compared to designs with channels distributed segmentally and centrally. This improved heat transfer can significantly benefit battery thermal management.

Another promising avenue for enhancing BTM involves the utilization of nanofluids, which are conventional coolants (such as water or ethanol) infused with nanoparticles like Al_2O_3 or CuO. This approach holds significant potential for improving heat transfer characteristics. Nanofluids achieve higher thermal conductivity compared to traditional coolants by incorporating nanoparticles into the base fluid, enabling more promising heat dissipation from batteries [23−25]. This attribute is particularly crucial for high-discharge-rate operations that generate considerable heat. Furthermore, nanofluids exhibit outstanding stability and suspension properties, effectively preventing particle settling and sedimentation. This ensures a durable and reliable cooling solution for EV batteries. Their compatibility with existing LCS also simplifies integration into current battery pack designs, making them an attractive option for the EV industry [26]. However, the literature on the performance of nanofluids in BTMS is limited [27]. This underscores the need for further research in this area to fully understand and optimize their effectiveness in enhancing BTMS.

Keeping in view of these authentic reports, modifications are hereby proposed to the mini-channel cooling arrangement within Wu et al. [19] design. This improved design has been designated by as Design 3. It incorporates a fully covered cooling plate with a serpentine flow pattern and shall be compared with Design 1 and Design 2. Adopting the initial comparison using water as the coolant, the use of nanofluids containing silver and copper oxide nanoparticles would be investigated. These nanoparticles are selected for their high thermal conductivity and less agglomeration and sedimentation effects, making them more favorable for efficient heat transfer in various thermal applications such as solar thermal collectors, etc., [28,29]. This study would particularly focus on crucial parameters such as the type of coolant (water vs. nanofluid), volume fractions (0.25% & 0.5%) and flow velocities to find out how promisingly each coolant improves temperature reduction within the proposed battery module (Design 3). Ultimately, it has been aimed to

compare the performance of these Designs namely 1, 2 & 3 and coolants to gain valuable insights into optimizing BTMS in EVs using a combination of innovative channel designs and nanofluids.

2. Methodology

2.1. Conceptual description

This study delves into thermal management strategies for a lithium iron phosphate ($LiFePO_4$) battery, a popular choice in electric vehicles due to its stability and longevity (3.2 V, 10 Ah, pouch-type configuration details are Provided in Table 1 [30]). The battery's key components — the anode and cathode tabs and the main body are visualized in Fig. 1 (a) & (b). Fig. 2 (a)-(c) showcases three distinct mini-channel LCS utilized for the analysis. Each system utilizes a pair of 3 mm thick aluminum (Al) cold plates to sandwich a single battery cell. These cold plates house mini-channels each with a precisely defined cross-sectional area of 2 mm × 6 mm. Tables 1 and 2 offers a comprehensive overview of these cooling systems including their 3D modeling and design specifications (created using CATIA software).

Table 1. Ideal values of battery parameters [30].

No	Key parameters of a battery	Typical values material deployed
1	Cathode	$LiFePO_4$
2	Anode	Graphite
3	Nominal voltage	3.2 V
4	Nominal capacity	10 Ah
5	Average density (kg m^{-3})	1881.45
6	Width (mm)	100
7	Length (mm)	115
8	Thickness (mm)	12

The core of this investigation lies in understanding how the arrangement of flow channels within the cold plates impacts cooling performance. Comparison of three designs is appended hereunder.

- **Design 1:** Introduced by Jia et al. [18]. This design utilizes partially encased cold plates with mini-channels distributed in a segmented and central configuration.
- **Design 2:** Building upon Design 1 and it employs full cold plate coverage, while maintaining the same mini-channel arrangement as established by the model of Wu et al. [19].
- **Design 3:** The proposed model of this work offers an improved design with full cold plate coverage featuring a serpentine flow pattern for the mini-channels. It is anticipated that this design would enhance temperature uniformity within the battery, providing valuable insights into optimizing cooling efficiency through flow channel arrangements.

2.2. Physical and mathematical models for the novel design of batteries

When a battery is being cycled or decycled, heat is generated inside the battery, mostly in the form of Joule heat and electrochemical reactions. This heat is vented outside or transmitted to surrounding cooling plates. It is well-identified that during high charge/discharge rates, the tabs typically reach their peak temperature. The heat created is transferred to the battery body, wherever the temperature is lower,

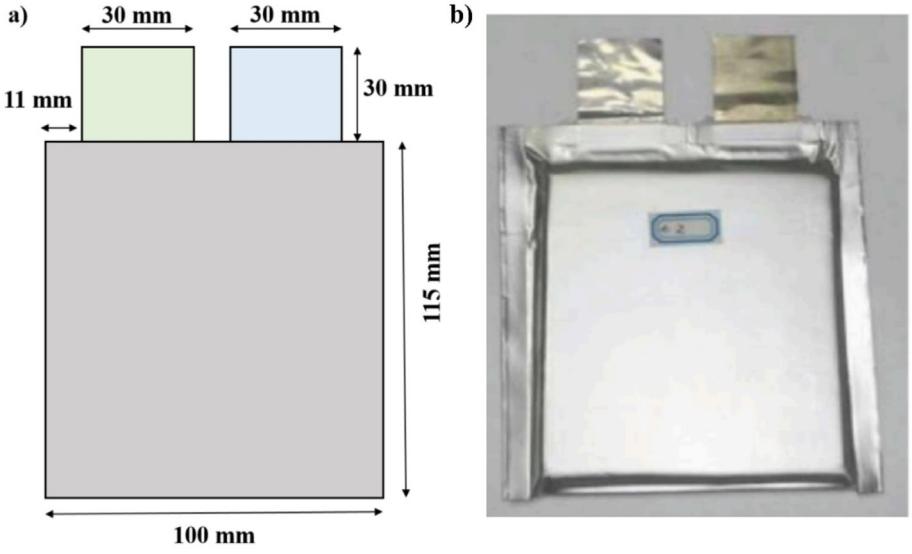

Fig. 1. a) Dimensions and b) Image of a pouch-type battery [19].

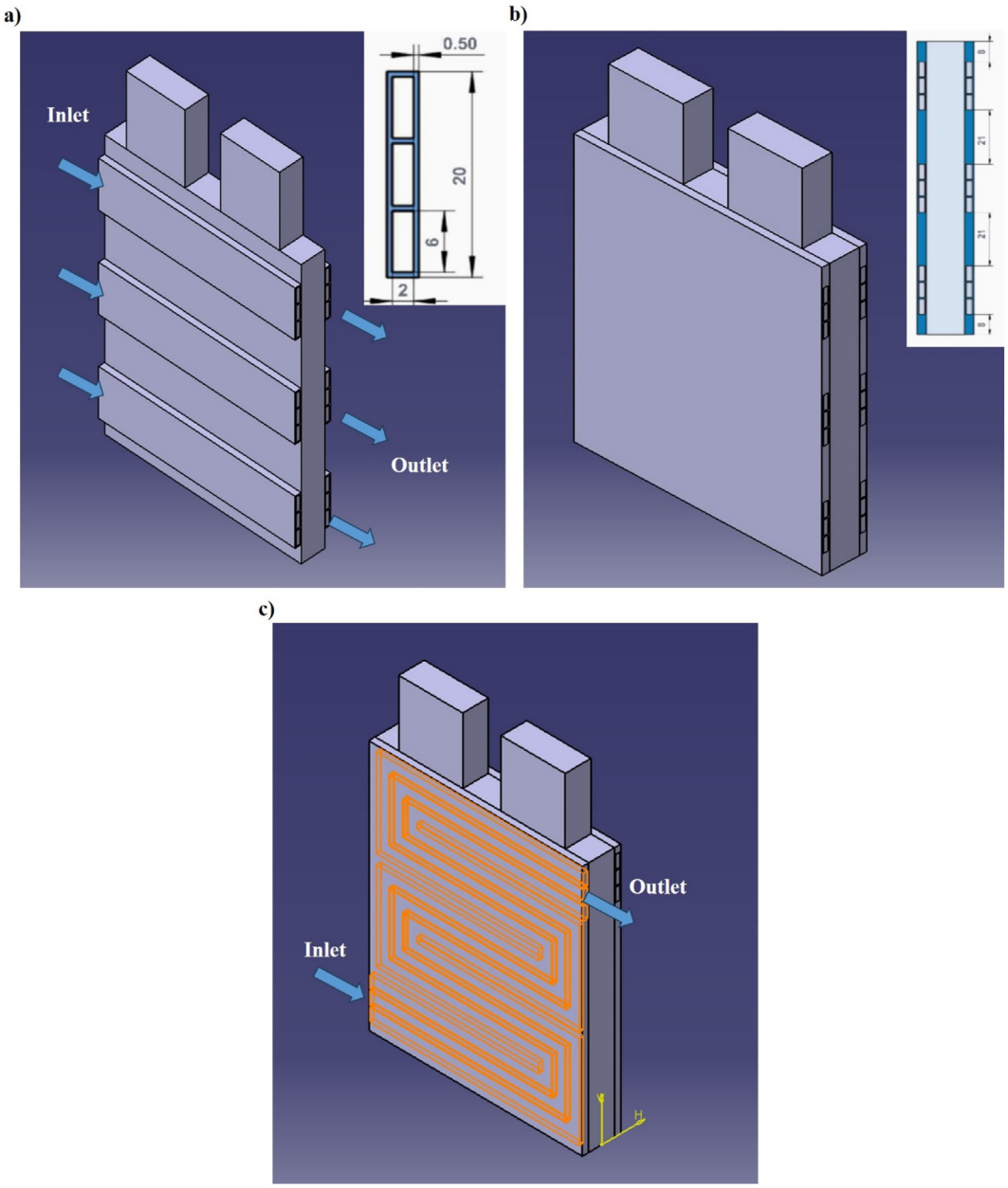

Fig. 2. Different type of mini-channel LCS architectures designed for the pouch type LIB; a) Design 1 [18]; b) Design 2 [19]; and c) Design 3 (Our proposed model).

Table 2. Comparison of battery design Configurations.

Configuration	Battery arrangement	Mini-channel integration	Cold plate placement
Design 1 (Jia et al. [18])	Partially encased cold plate	Mini-channels distributed segmentally and centrally.	Partially encase the battery surface and directly contact with mini channels.
Design 2 (Wu et al. [19])	Fully covered cold plate	Same as Design 1.	Fully covers the battery surface and directly contact with mini channels.
Design 3 (Our work)	Fully covered cold plate	Serpentine flow pattern (3 flat tubes) can help to maximize the contact area between the cooling fluid and the cold plate, improving heat transfer efficiency.	Fully covers the battery surface and directly contact with mini channels.

simultaneously blocking the battery cores heat dissipation channel. As a result, the tab temperature is also considered in this study as it plays a crucial role in the TM of battery cells. Liquid water serves as the cooling fluid in this study; water enters the system from the left (next to the positively charged electrode, where the most heat output occurs). Before exiting the battery system at the outlet, the coolant absorbs high temperature from the battery system, including the heat from the cold plates. Four different subdivisions have been established inside the present computational domain: cold plate, minichannel, positive and negative tabs and the battery body. These subdivisions play a crucial role in providing a quantitative explanation of the pertinent fluid and heat transport processes. The numerical equations are detailed in Table 3 and their explanations are provided hereunder.

1. **Cold plate:** This component, typically constructed from aluminum due to its excellent thermal conductivity and it plays a vital role in heat dissipation. Heat transfer within the cold plate is governed by transient Fourier's law, applicable to solid structures.
2. **Mini-channels:** A network of mini-channels facilitates the efficient flow of coolant throughout the battery system. A constant mass flow rate of liquid water is introduced into these channels. Reynolds number calculated using Equation (1), characterizes the flow regime within the mini-channels and it is given by;

$$Re = \frac{\rho_f u D_h}{\mu_f} \tag{1}$$

where: Re = Reynolds number, ρ_f = Density of coolant (water), u = Velocity of coolant, D_h = Hydraulic diameter of channel (assumed 3 mm in this study) and μ_f = Dynamic viscosity of coolant (water). Based on the highest flow rate employed (1×10^{-3} kg/s), the Reynolds number is approximately 286, indicating laminar flow within the mini-channels.

3. **Positive and Negative tabs:** These current collectors constructed from copper and aluminum respectively due to their high conductivity, generate heat through ohmic resistance. Equation (2) outlines the determination of the heat generation rate in the tabs:

$$q_{Al/Cu} = \frac{Q_{Al/Cu}}{V_{Al/Cu}} = \frac{I^2 R_{Al/Cu}}{V_{Al/Cu}} \tag{2}$$

where: $Q_{Al/Cu}$ = Tabs heat generation rate, $R_{Al/Cu}$ = Tabs resistance, $V_{Al/Cu}$ = Tabs volume and I = Current flow.

4. **Battery body:** Heat generation within the battery body is calculated using the Bernardi equation (given in Equation (3)), which incorporates dynamic variations in battery temperature, resistance and voltage coefficients.

$$q_b = \left(I^2 R_b - IT \frac{dU}{dT} \right) / V_b \tag{3}$$

where: q_b = Battery body heat generation rate, R_b = Battery body resistance (temperature dependent), $\frac{dU}{dT}$ = Dynamic voltage temperature coefficient, T = Battery temperature and V_b = Battery body volume.

To achieve a precise temperature distribution, it is imperative to accurately specify thermophysical parameters. The thermophysical properties of these battery body materials are homogenized and considered

Table 3. Governing equations [31,32].

Areas of computation analysis	Equations
For positive, negative tab	Energy equation $\rho_{Al/cu} C_{P,Al/cu} \frac{\partial T_{Al/Cu}}{\partial t} = \nabla \cdot (k_{Al/cu} \nabla T_{Al/Cu}) + q_{Al/Cu}$
Battery body	Energy equation $\rho_b C_{P,b} \frac{\partial T_b}{\partial t} = \nabla \cdot (k_b \nabla T_b) + q_b$
Cold plate	$\rho_c C_{P,c} \frac{\partial T_c}{\partial t} = \nabla \cdot (k_c \nabla T_c)$
Coolant flow	Mass equation $\frac{\partial \rho_f}{\partial t} + \nabla \cdot (\rho_f \vec{u}) = 0$ Momentum equation $\frac{\partial}{\partial t}(\rho_f \vec{u}) + \nabla \cdot (\rho_f \vec{u} \vec{u}) = -\nabla_P$ Energy equation $\rho_f C_p, f \frac{\partial T_f}{\partial t} + \nabla \cdot (\rho_f C_{p,f} \vec{u} T_f) = \nabla \cdot (k_f \nabla T_f)$

constant to facilitate computation [33]. Table 4 provides detailed information regarding the thermophysical characteristics of these materials and they are used in the present simulations.

2.3. Thermophysical characteristics of proposed nanofluid

Thermal management is a critical aspect of lithium-ion battery design, as excessive heat generation can significantly impact performance and their lifespan. This study explores the potential of nanofluids and suspensions of nanoparticles in a base fluid by deeming it as a novel approach to improve battery thermal management by the way utilizing the proposed battery designated as “Design 3”. Owing to the high thermal conductivity of nanoparticles, it can significantly enhance the heat transfer capabilities of the base fluid. Herein, the study of use of silver (Ag) and copper oxide (CuO) nanoparticles dispersed in water to create nanofluid coolants has been made. These specific nanoparticles were chosen for their favorable thermal-physical characteristics, including high thermal conductivity and good corrosion resistance making them well-suited for battery applications.

Nanofluid coolants were prepared with silver and copper oxide nanoparticles at the preferred volume concentrations of 0.25% and 0.5%. These concentrations was selected, based on previous relevant research made by Wiriyasart et al. [34] and the same has been corroborated in this work, whenever applicable and appropriate. It has been demonstrated that higher concentrations of nanofluids are more effective in maintaining lower battery temperature. As the nanoparticle concentration increases, several factors contribute to this enhanced cooling capacity. These include improved thermal conductivity of the nanofluid, increased surface area for heat transfer and more frequent molecular collisions within the fluid.

For a computational modeling purposes, the nanofluid is considered as a homogeneous liquid with effective properties that capture its overall heat transfer behavior. This simplification facilitates the use of established heat transfer equations. It is to be noted that the equations employed in this work is to describe the conservation of mass, momentum and energy within this effective nanofluid. To ensure accurate results, selecting the most appropriate correlation for determining crucial nanofluid parameters, particularly thermal conductivity, which is quite essential for a battery. These correlations account for the properties of both the nanoparticles and the base fluid. The specific equations used for calculating the key thermal-physical properties (thermal conductivity, density, specific heat and viscosity) of the silver/copper oxide-water nanofluids employed in this study are summarized in Table 5. In addition, Table 6, presents the relevant parameters for the chosen nanoparticles and water.

Table 4. Physical and thermal properties of the LIBs materials used in numerical modeling.

No	Material	Density, (kg/m^3)	Thermal conductivity, (W/mK)	Heat capacity, (J/kg K)
1	Battery	1881.4	(x,y)1.35; (z) 0.98	2520
2	Aluminium	2719	202.4	871
3	Copper	8978	387.6	381
4	Liquid water	998.2	0.6	4182

2.4. Boundary conditions and initialization

In this computational modeling, a constant discharge rate of 5C is employed, assuming the designed battery model fully depletes within 720 s. The boundary conditions are defined for coolant entrance and outflow within the mini-channels. For coolant flow, mass flow inlet boundaries are implemented at the points, where coolant enters the mini-channels, while pressure outlet boundaries are used for the coolant exiting. The inlet mass flow rate is varied from 1×10^{-6} kg/s to 1×10^{-3} kg/s to simulate different cooling scenarios. The pressure at the outflow is set to zero Pascal. Boundaries between distinct subdomains like those between the battery body and cold plate, tabs & cold plate and cold plate & mini-channels are designated as thermal coupled interfaces. In this analysis, the impact of thermal contact resistance is not taken account. Similar kind of observations were made earlier [19] which stood as the foundation for this work. Natural convection boundary conditions are applied to the external surfaces of the cold plate and battery. These conditions are empirically represented by a convective heat

Table 5. Equations for the properties of nanofluids [35].

No.	Properties	Numerical equations
1	Density (ρ)	$\rho_{nf} = (1-\phi)\rho_{bf} + \phi\rho_{np}$
2	Specific heat (C_p)	$\rho_{nf}c_{nf} = (1-\phi)\,(\rho c_P)_{bf} + \phi(\rho c_P)_{np}$
3	Dynamic viscosity (μ)	$u_{nf} = \mu_{bf}(1+2.5\phi)$
4	Thermal conductivity (K)	$k_{nf} = \frac{k_{np}+2k_{bf}+2(k_{np}-k_{bf})\phi}{k_{np}+2k_{bf}-2(k_{np}-k_{bf})\phi}k_{bf}$

Table 6. Properties of nanoparticles and water [36,37].

S.No	Coolants	Silver (Ag)	Copper oxide (CuO)	Water
1	Density, ρ	10,490 kg/m^3	6500 kg/m^3	998.2 kg/m^3
2	Specific heat, C_p	710 J/kg.K	551 J/kg.K	4128 J/kg.K
3	Thermal conductivity, k	429 W/m.K	32.9 W/m.K	0.6 W/m.K

transfer coefficient of 5 W/(m^{2}K). To ensure consistency across all simulations, a uniform initial temperature of 300 K is applied throughout all computational domains and the external environment.

3. Mesh testing and validation

In this analysis, a structured mesh was generated using CFD ANSYS Fluent for Design 2. To assess grid independence and the influence of mesh density on numerical results, three distinct mesh techniques are employed; Each with varying element counts: 238,401 elements (Mesh 1), 424,417 elements (Mesh 2) and 487,195 elements (Mesh 3). Particularly, Design 2 was applied for this analysis corresponding to the model of Wu et al. [19] allowing validation with available reports.

To quantify the impact of mesh density on the numerical results, the maximum battery temperature under water cooling was monitored. A constant water flow rate of 2 $\times$ 10^{-5} kg/s and a discharge rate of 5C as proposed in the literature [19] were used for this analysis. The maximum temperature obtained with each mesh are presented in Fig. 3. A pre-defined convergence criterion based on the relative change in maximum temperature between subsequent mesh refinements was employed. Results from Meshes 2 and 3 exhibited minimal deviation, indicating grid independence. Consequently, Mesh 2 was chosen for subsequent simulations due to its optimal balance between accuracy and computational efficiency.

For further validation of the present numerical approach, a comparative analysis was conducted with the findings reported in the literature [19] for their Design 2 (Fig. 4). The maximum battery temperature obtained with Mesh 2 under identical operating conditions (5C discharge rate, water coolant) was compared

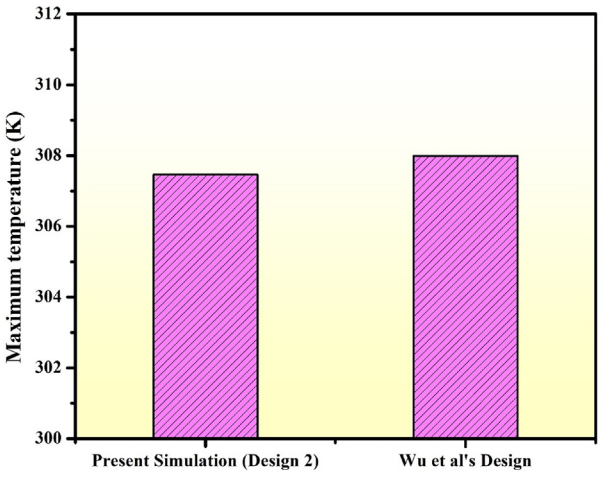

Fig. 4. Validation of Design 2 with results reported by Wu et al. [19].

to their results. The maximum battery temperature predicted by the present model for Design 2, which is similar to the work of Wu et al. model, exhibited excellent agreement with their reported values [19]. This validation confirms the accuracy of our mesh generation and simulation setup for pouch battery modeling. Furthermore, this level of accuracy justifies applying the established mesh parameters (element size, refinement strategy) to this improved Design 3, that incorporates an innovative minichannels arrangement (serpentine flow pattern) with three inlets and three outlets for enhanced thermal management.

4. Results and discussions

4.1. Water as coolant

In this section, the cooling performance of three pouch-type battery designs (Designs 1, 2 and 3)

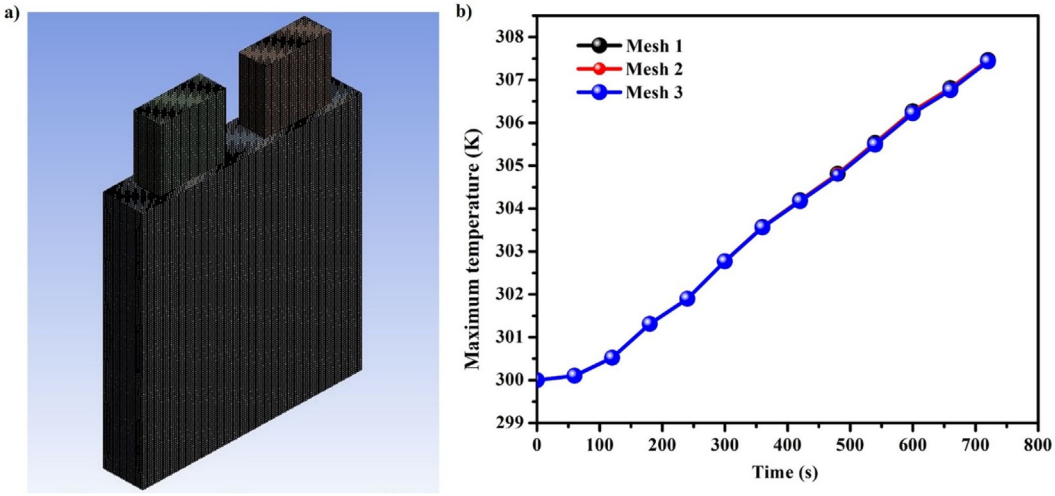

Fig. 3. (a) Structured grid mesh (b) Variation of the battery surface temperature in Design 2.

featuring different minichannel arrangements is investigated under a demanding 5C discharge condition. A validated numerical approach was employed to assess the thermal performance of each design. Water, a common choice due to its cost-effectiveness and wide availability, was initially selected as the coolant at a flow rate of 2×10^{-5} kg/s for all designs. This selection aligns with the literature [19] to facilitate a direct comparison. This initial flow rate served as a baseline for evaluating the relative cooling effectiveness of each minichannel configuration. The findings highlight the significant influence of minichannel arrangement on battery thermal management. Design 1, featuring a partially covered cold plate, exhibited the least effective cooling performance (shown in Figs. 5 and 6). This incomplete coverage resulted in uneven heat distribution across the battery surface leading to a peak temperature of 310.9 K by the end of the discharge process ($t = 720$ s). As illustrated in Fig. 6, Design 1 suffers from pronounced temperature stratification with areas directly exposed to the environment experiencing significantly higher temperatures compared to regions in contact with the cold plate. This inadequate heat dissipation across the entire battery surface translates to poorer in-plane temperature uniformity, a critical factor for battery health and performance.

In contrast, Design 2 demonstrated a marked improvement in cooling performance compared to Design 1. This improvement can be attributed to the implementation of a fully-covered cold plate with segmented mini-channels. The full coverage ensures more consistent heat transfer from the battery cells to the coolant, while the segmented mini-channels enhance fluid flow characteristics and promote better heat removal. These combined factors lead to a reduction in temperature spikes and a more uniform temperature distribution across the battery surface. By the end of the discharge process, Design 2 achieved a lower peak temperature of 307.4 K compared to Design 1.

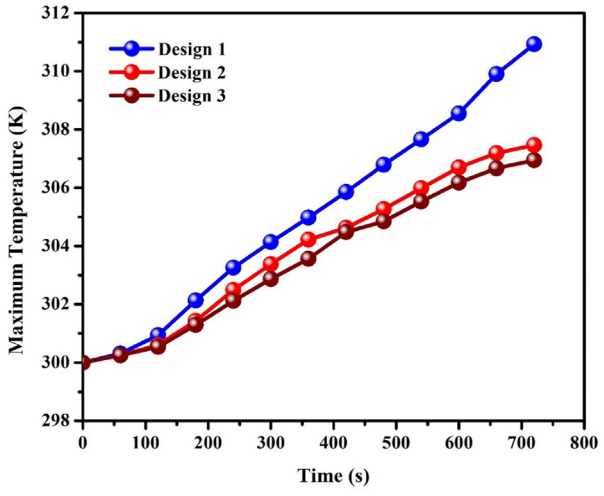

Fig. 5. Temporal variation of the maximum surface temperature for the three battery designs at a coolant mass flow rate of 2×10^{-5}kg/s using water as the coolant.

It is pertinent to note that Design 3 emerged as the superior design in terms of cooling efficiency, achieving exceptional thermal management capabilities. Similar to Design 2, it incorporates a fully-covered cold plate. However, Design 3 utilizes serpentine flow pattern mini-channels, which likely to contribute for its superior cooling performance. It has demonstrated exceptional thermal management capabilities and established itself as a benchmark for conventional water-cooling approaches. Furthermore, it was found that it helped to maintain the battery surface temperature within the specified operating range of the batteries and did not lead to the thermal runaway or degradation.

It has been witnessed that the findings from the simulations for Designs 1 and 2 closely align with the reported simulation results in the literature [19] for the same designs employing water as the coolant, confirming the validity and robustness of the present three designed models. Thus, Design 3 consistently outperforms its counterparts in thermal management while using water coolant compared to Designs 1 and 2. This superior performance provides the greatest trust and extends to the utilization of two distinct nanofluids: one infused with Ag nanoparticles and the other with CuO, both utilizing water as the base fluid.

This study also investigates the influence of coolant mass flow rate on the cooling performance of BTMS within Design 3. The coolant mass flow rate was varied from 1×10^{-6} kg/s to 1×10^{-3} kg/s so as to assess its impact on both cooling efficiency and pressure drop (Fig. 7 a) and b)). The results demonstrate a strong correlation between coolant flow rate and battery thermal management. Our analysis revealed a significant decrease in maximum battery temperature with increasing coolant flow rate. This reduction was mostly pronounced at lower flow rates ($m_f < 6 \times 10^{-4}$ kg/s). While further increase in flow rate has resulted in continued temperature reduction. The effect became progressively smaller. This trend suggests a point of diminishing returns, where additional pumping power required for higher flow rates may not be justified by the marginal gains in cooling performance. At a flow rate of 6×10^{-4} kg/s, the coolant effectively removes heat from the battery cells, leading to a significant decrease in the maximum temperature observed. This reduction contributes to a more uniform temperature distribution throughout the battery and this also serves as a crucial factor for maximizing battery lifespan and overall system performance.

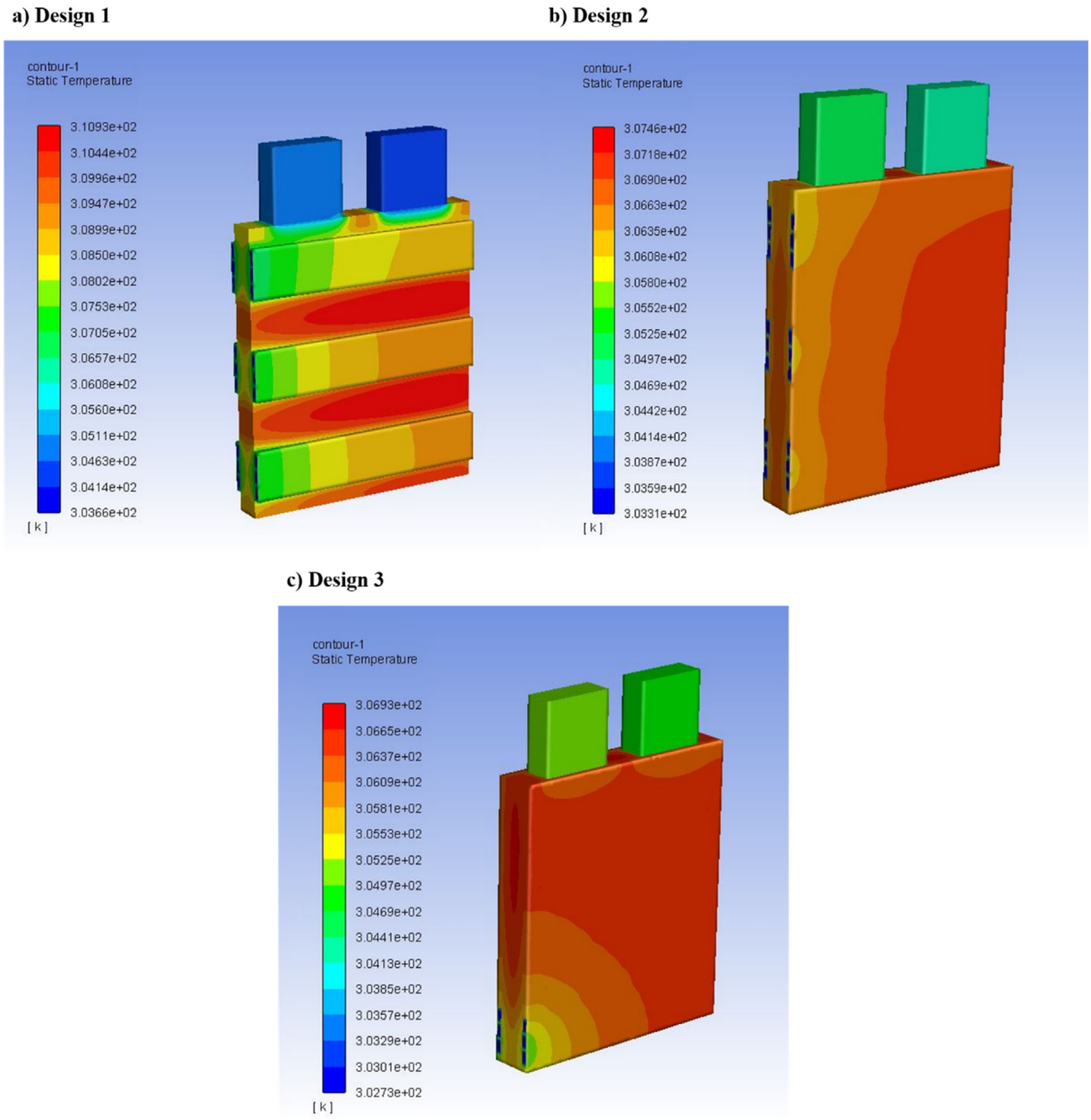

Fig. 6. Temperature contours of the battery body for the (a) Design 1, (b) Design 2 and (c) Design 3 at 720 s under a 5C discharge rate with water serving as the coolant at a mass flow rate of 2 × 10⁻⁵kg/s.

It is important to acknowledge the interplay between flow rate and pressure drop within the cooling channels. As illustrated in Fig. 7 (b), higher flow rates lead to increased pressure drop due to the greater resistance encountered by the coolant as it travels through the channels. Minimizing pressure drop is critical for reducing pumping power consumption and enhancing the overall energy efficiency of the BTMS. The pressure drops observed in the simulations for Design 3 are deemed acceptable. Similar trends have been reported in the literature [38]. This is particularly noteworthy because the implemented cooling channel design effectively mitigates the pressure rise associated with higher flow rates. Based on this analysis, a flow rate of approximately 6×10^{-4} kg/s appears to be a favorable compromise. It achieves a substantial temperature reduction while maintaining acceptable pressure drop and associated energy consumption.

4.2. Impact of silver and CuO nanoparticle based nanofluids on battery cooling performance

In this section, the influence of silver nanoparticle (Ag)-based nanofluids at concentrations of 0.25% and

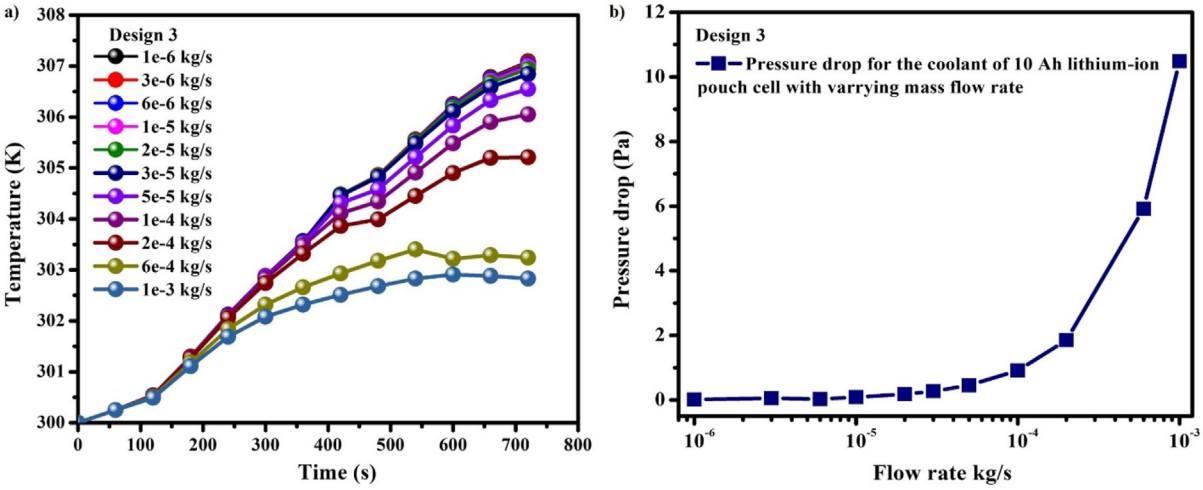

Fig. 7. a) Variations in battery surface temperature and b) pressure drop with changes in coolant velocity for Design 3.

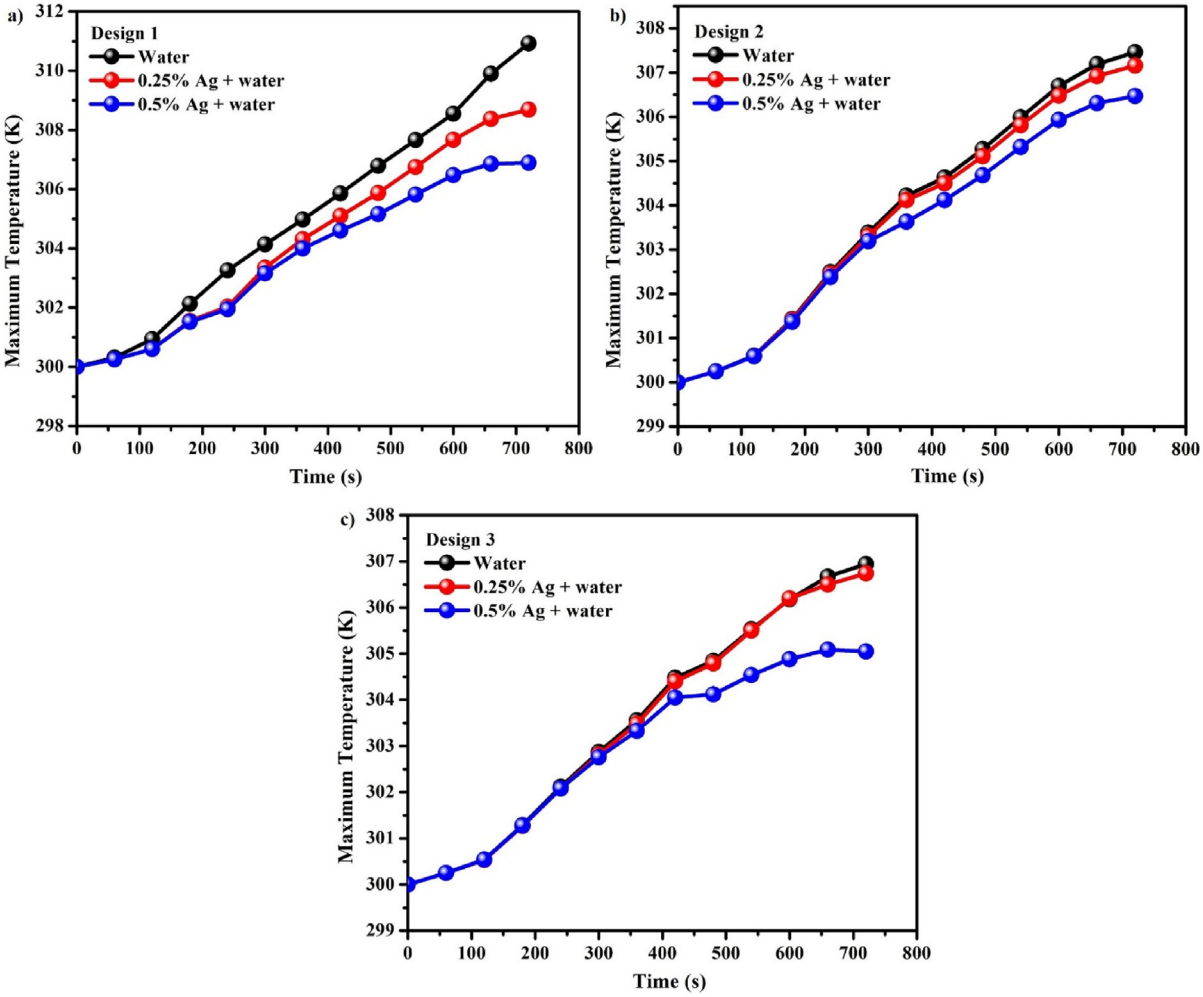

Fig. 8. Effects of Silver nanofluid concentrations (0.25% & 0.5% VF) on a) Design 1, b) Design 2 and c) Design 3.

0.5% (by volume fraction) on battery cooling performance in Designs 1, 2 and 3 has been investigated using a numerical analysis. Deionized water served as the base fluid. The inclusion of Ag nanoparticles enhanced the thermal properties of the coolant, particularly its thermal conductivity. In addition, brownian motion of the nanoparticles intensified heat transfer within the nanofluids compared to plain water. Silver nanoparticles were chosen for their unique properties including high thermal conductivity making them suitable for efficient heat transfer in various thermal applications. Initially, Ag nanofluid was introduced into Designs 1 and 2 to evaluate its impact. Design 1 achieved maximum cell temperatures of 308.6 K and 306.8 K (Fig. 8) with 0.25% and 0.5% Ag nanofluid, respectively representing a 2.8% and 2.2% increase from the initial battery temperature (300 K). While these results indicate improvement over water cooling (310.9 K), but their performance is inferior to Design 3.

When introduced into Design 3, the 0.25% and 0.5% Ag nanofluid yielded maximum cell temperature of 306.7 K and 305.0 K (Fig. 8), respectively. These values

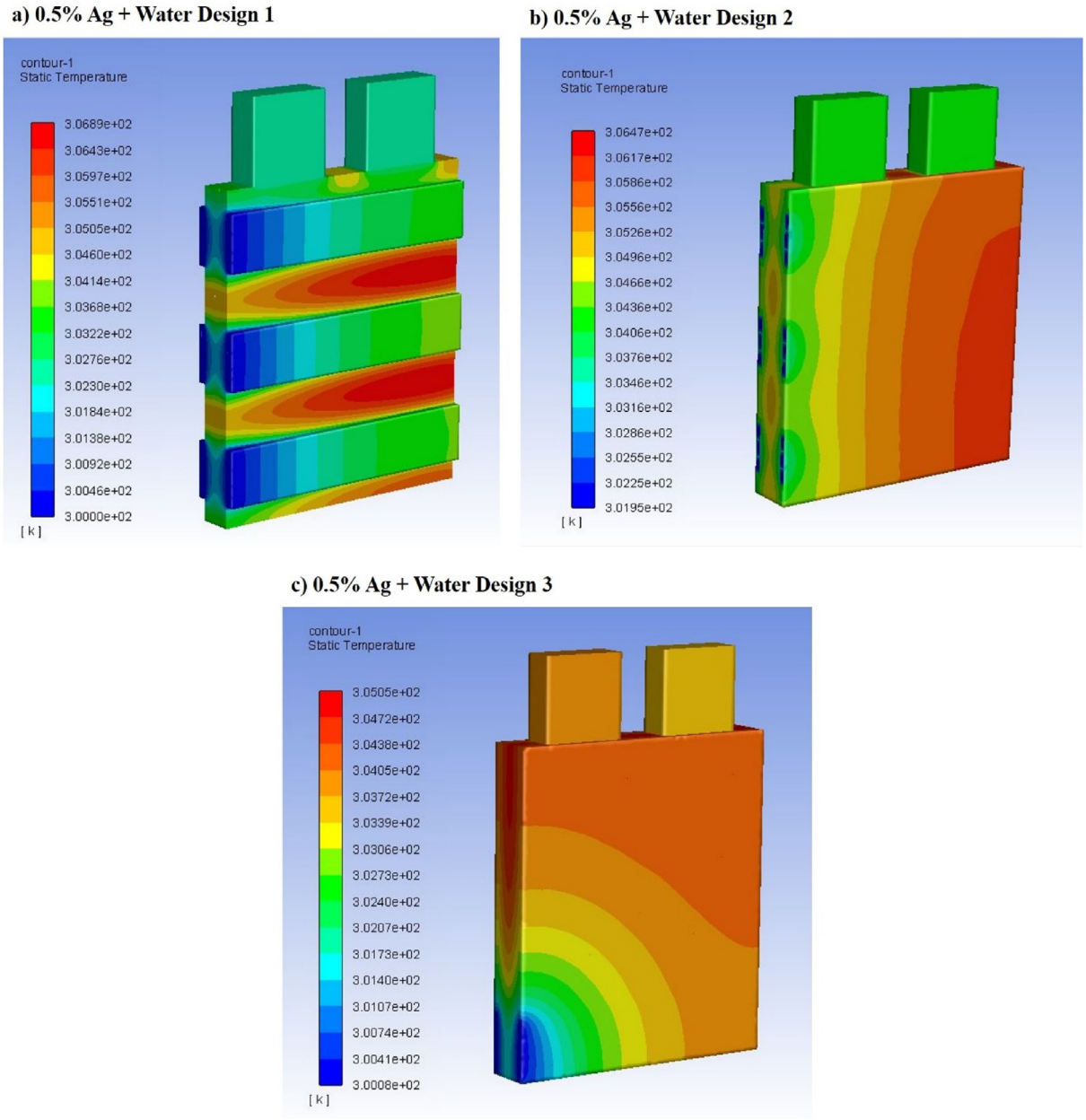

Fig. 9. Temperature distribution in battery designs (a) 1, (b) 2 and (c) 3 when using 0.5% VF Ag based nanofluid.

are only 2.1% and 1.6% higher than the initial temperature demonstrating a significant improvement compared to Designs 1 and 2 and water cooling. This consistent reduction in cell temperature across concentrations underscores the effectiveness of Ag nanofluids in achieving uniform cooling within Design 3. It also suggests a trend of improved cooling performance with higher nanofluid concentrations (0.5% Ag). The temperature distributions of battery Designs 1, 2 and 3, when using 0.5% VF Ag are shown in Fig. 9. The results of this analysis demonstrate the capability of using Ag nanoparticle-based nanofluids as an effective coolant for BTM, particularly in Design 3. This improved thermal management capability offered by nanofluids can contribute to maintaining lower battery temperatures, thereby enhancing the performance and life cycle of the battery. These findings are consistent with existing literature on silver nanoparticle-water nanofluids, which have been identified as promising candidates for efficient thermal conduction in various applications [39−41]. Furthermore, Ag- nanoparticles exhibit good thermal stability, approximately up to 313 °C, making them suitable for long-term use in BTMS of EVs [42].

Furthermore, Design 3 incorporates a serpentine flow pattern of mini-channels within the cold plate, while Designs 1 and 2 utilize parallel and segmented mini-channel arrangements. This serpentine flow pattern offers several advantages for heat transfer and fluid dynamics within the battery module. The serpentine flow promotes more efficient fluid flow characteristics by increasing the fluid-cell contact time, allowing for better heat dissipation from the cells to the coolant and leading to more effective cooling. The serpentine flow pattern also facilitates uniform distribution of the coolant across the battery surface, minimizing hotspots and reducing thermal gradients throughout the battery [43,44].

Similarly, the impact of copper oxide nanoparticle-based nanofluids on battery cooling performance in

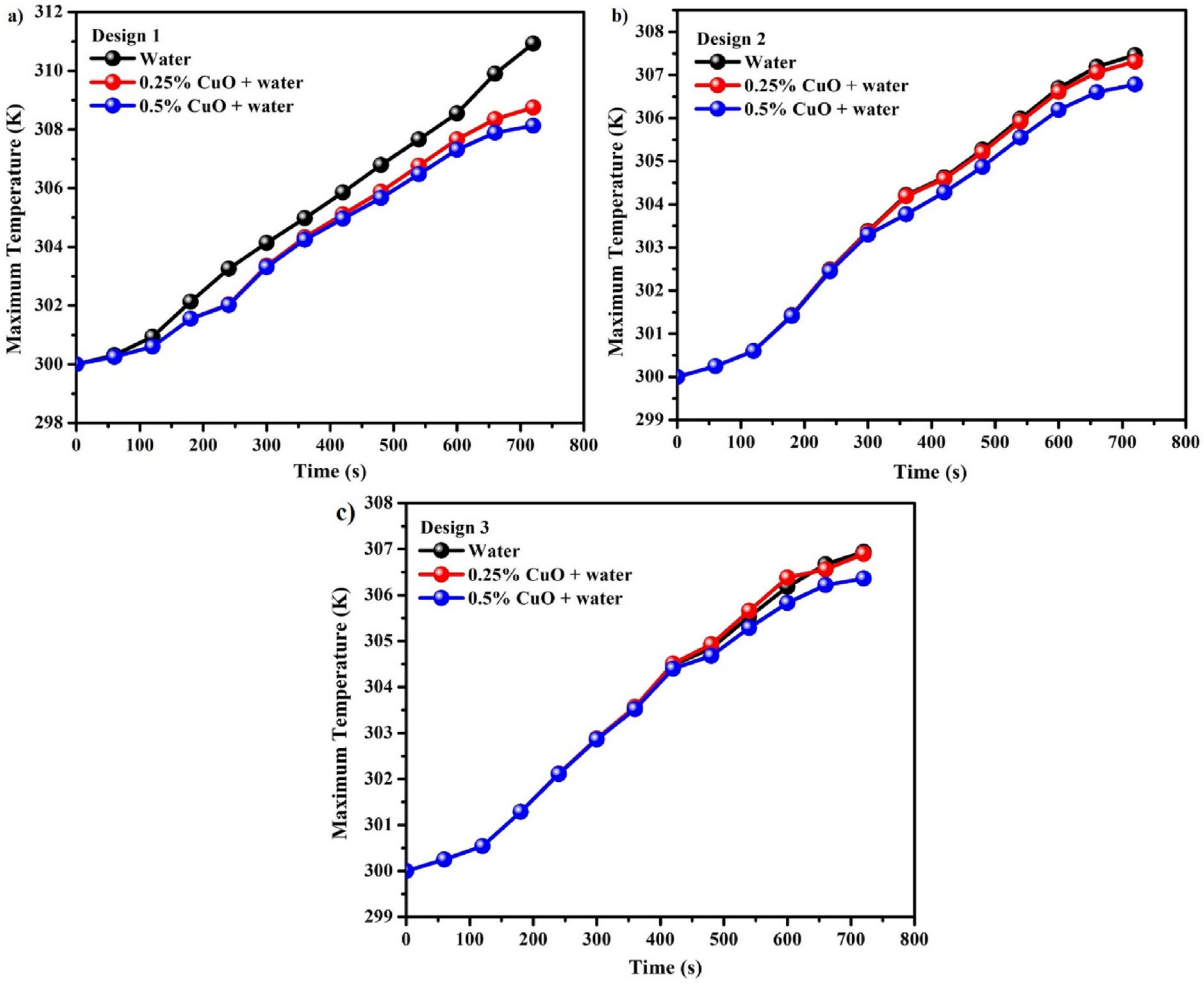

Fig. 10. Impact of copper oxide nanofluid concentrations (0.25% and 0.5% VF) on the thermal management performance of battery models a) 1, b) 2 and c) 3.

Designs 1, 2 and 3 was evaluated with two different CuO nanofluid concentrations of 0.25% and 0.5% VF. CuO nanoparticles were chosen for their high thermal conductivity, stability at elevated temperature and uniform heat dissipation properties. When introduced into all three Design, CuO nanofluids exhibited maximum cell temperature of 306.9 K and 306.3 K (Figs. 10 and 11) for concentrations of 0.25% and 0.5% VF respectively, slightly lower than upon using water as the coolant. Notably, Design 3 with CuO nanofluid (0.5% VF) maintained excellent cooling performance but was inferior to Design 3 using silver nanofluid. Fig. 12 demonstrates a graphical comparison of the thermal management performance of Designs 1, 2 and 3 using water, Ag-based nanofluid and CuO-based nanofluid as coolant.

This performance disparity can be attributed to several factors inherent to the nanoparticles. Silver nanoparticles typically possess higher thermal conductivity and smaller particle sizes compared to CuO nanoparticles resulting in larger surface areas for improved heat transfer efficiency. Particularly, Ag nanoparticles exhibit better dispersion characteristics and chemical stability in water-based fluids, ensuring long-term effectiveness as coolants [45,46]. Furthermore, Design 3 features an innovative serpentine flow

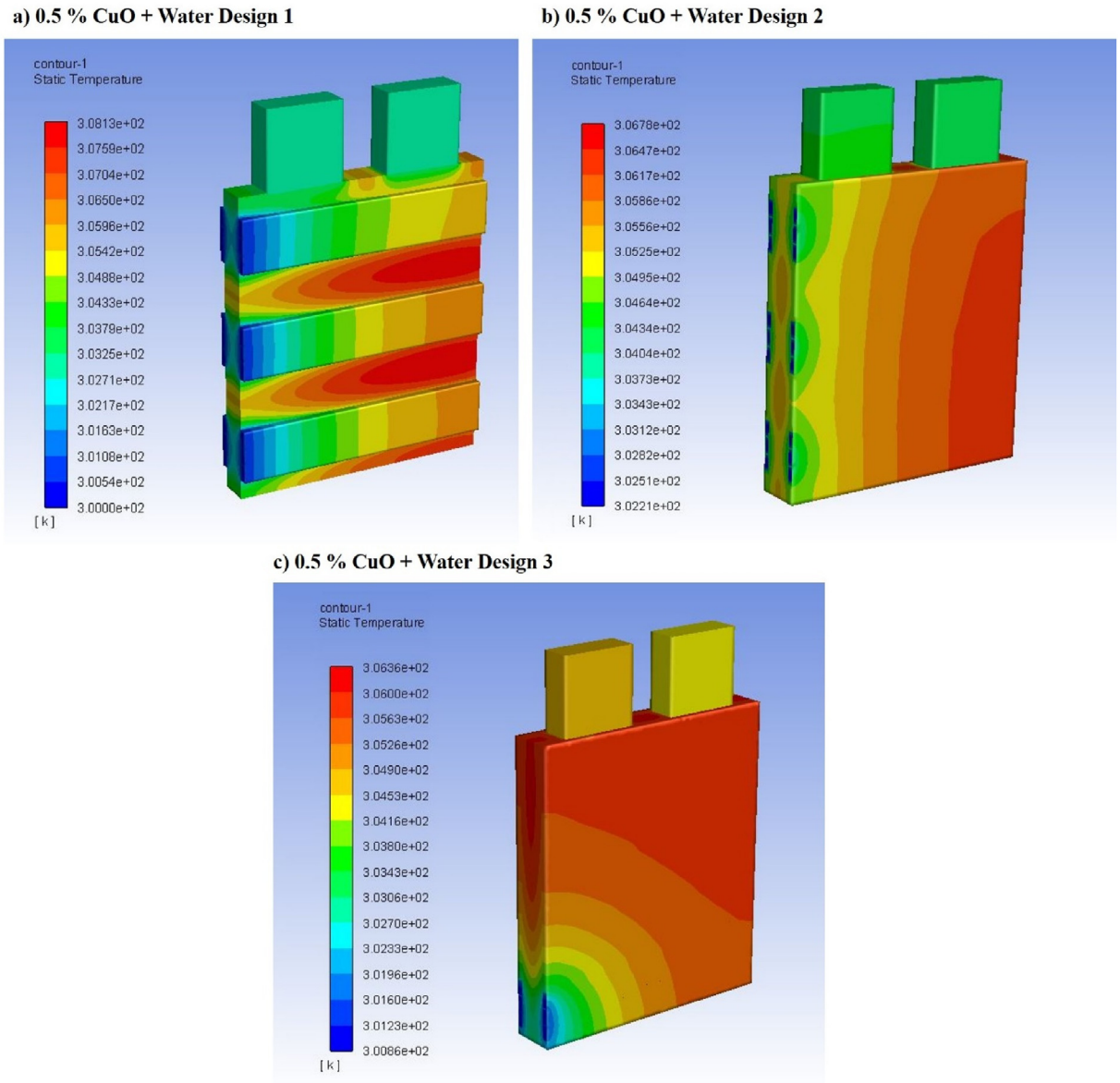

Fig. 11. Temperature distribution in battery designs a) 1, b) 2 and c) 3 when using 0.5% VF CuO based nanofluid.

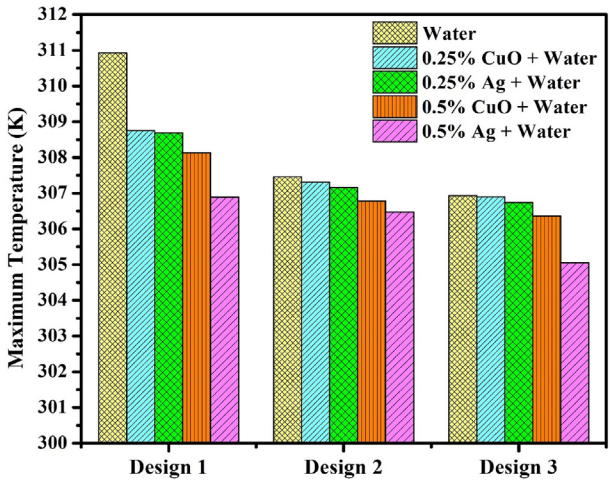

Fig. 12. Graphical comparison of the thermal management performance of Design 1, 2, and 3 using water, Ag-based nanofluid and CuO-based nanofluid as coolant.

pattern of mini-channels covered by the cold plate, whereas Designs 1 and 2 contain parallel and segmentally arranged mini-channels. This innovative flow pattern in Design 3 enhances fluid flow characteristics and promotes better heat removal contributing to its superior cooling performance with silver nanofluids. Table 7 represents the comparison of temperature of the cell for Designs 1, 2 and 3 by utilizing different type of coolants.

Conversely, copper oxide nanoparticles may experience greater tendencies for agglomeration and reactivity in aqueous solutions, potentially limiting their heat transfer capabilities and stability over time [47,48]. Consequently, Ag nanoparticle-based nanofluids demonstrate superior performance in battery cooling applications due to their enhanced thermal conductivity, dispersion, stability characteristics and the innovative flow pattern employed in Design 3. Despite the relatively modest temperature reductions compared to water, CuO nanofluids still show promise for enhancing heat transfer and contributing to the longevity of electric vehicle batteries.

Succinctly, findings of this work, demonstrate that silver nanofluids significantly enhance thermal management performance, particularly when used in Design 3 with its serpentine flow pattern. This improvement is evident when compared to water cooling, CuO nanofluids and even Design 1 and 2 and it also emphasizes the critical role of both nanofluid properties and battery design, in achieving optimal thermal management.

Table 7. Comparison of temperature of the cell for Designs 1, 2 and 3 with different types of coolants.

Design No.	Coolant	Maximum Temperature (K)	Temperature difference (CuO vs water) (K)	Temperature difference (Ag vs water) (K)
1	Water	310.9	–	–
1	0.25% VF CuO	308.7	2.2	–
1	0.5% VF CuO	308.1	2.8	–
1	0.25% VF Ag	308.6	–	2.3
1	0.5% VF Ag	306.8	–	4.1
2	Water	307.4	–	–
2	0.25% VF CuO	307.3	0.1	–
2	0.5% VF CuO	306.7	0.7	–
2	0.25% VF Ag	307.1	–	0.3
2	0.5% VF Ag	306.4	–	1
3	Water	307	–	–
3	0.25% VF CuO	306.9	0.1	–
3	0.5% VF CuO	306.3	0.7	–
3	0.25% VF Ag	306.7	–	0.3
3	0.5% VF Ag	305.0	–	2

5. Conclusion

In this work, numerical demonstration of promising mini-channel LCS has been proposed for the thermal management of pouch-type LIBs. In addition, it has been highlighted the capability of using Ag and copper oxide nanoparticle-based nanofluids as effective coolants for BTM when compared to the traditional cooling approach. Some main conclusions are summarized below:

(i) Based on the analysis, it was explored that Design 3, featuring a three-inlet and outlet channel along with a serpentine flow pattern, demonstrated effective thermal management across a battery cell compared to Design 1 and Design 2, in both traditional water and nanofluid cooling approaches.

(ii) **Design 1 vs. Design 2 vs. Design 3 (Water-based coolant):** In Design 1, due to the partial coverage of the cold plate on the battery surface, it exhibited the weakest cooling performance. The maximum temperature in Design 1 increased to 310.9 K during the discharge process, resulting in poor temperature uniformity. At the same time, Design 2 demonstrated a marked improvement in cooling performance when compared to Design 1. This improvement can be attributed to the implementation of a fully-covered cold plate with segmented mini-channels. The full coverage ensures more consistent heat transfer from the battery cells to the coolant, while the segmented mini-channels enhance fluid flow characteristics and promote better heat removal. By the end of the discharge process, Design 2 achieved a lower peak temperature of 307.4 K compared to Design 1. However, Design 3, featuring a mini-channel system containing a favorable serpentine flow pattern and a fully covered cold plate, demonstrated the optimal cooling performance by reducing variations in temperature and enhancing temperature uniformity. Over the 5C discharge process, the maximum battery temperature was reduced to 307 K respectively. It is clearly established that Design 3, even when using water as the coolant displayed exceptional thermal management capabilities compared to Design 1 and Design 2. Thus, the design 3 would serve as a benchmark for conventional water-cooling approaches.

(iii) **Nanofluids-based cooling approach:** When 0.25% and 0.5% Ag nanofluid were introduced into Designs 1 and 2, the maximum cell temperatures reached 308.6 K, 306.8 K (Design 1) and 307.1 K, 306.4 K (Design 2), respectively, which was better than the water-cooling approach, where the maximum cell temperature reached 310.9 K and 307.4 K. However, in Design 3, the maximum cell temperature reached 306.7 K and 305.0 K for 0.25% and 0.5% Ag nanofluid, respectively demonstrating that Design 3 was superior in thermal management compared to Designs 1 and 2. The findings underscored the efficacy of employing Ag-nanoparticle-infused nanofluids as efficient coolants for BTM, particularly within the context of Design 3. Utilizing Ag nanofluids as coolants in Design 3 resulted in a notable decrease in the maximum surface temperature of the battery when compared to employing water as the coolant. This advancement in cooling efficiency was ascribed to the superior thermal conductivity and heightened molecular collisions facilitated by the expanded surface area of Ag- nanoparticles. Furthermore, Design 3 incorporates a serpentine flow pattern of mini-channels within the cold plate, while Designs 1 and 2 utilize parallel and segmented mini-channel arrangements. The serpentine flow pattern offers several advantages for heat transfer and fluid dynamics within the battery module. The serpentine flow promotes more efficient fluid flow characteristics by increasing the fluid-cell contact time allowing for better heat dissipation from the cell to the coolant and leading to more effective cooling. It also facilitates uniform distribution of the coolant across the battery surface, minimizing hotspots and reducing thermal gradients throughout the battery.

(iv) Similarly, when 0.25% and 0.5% CuO nanofluid were introduced into Design 3, the maximum cell temperature reached 306.9 K and 306.3 K, respectively which was only slightly lower than the temperatures when using water as the coolant in Design 3 as well as superior to Designs 1 and 2 operated under the same operating conditions. But it also proved inferior to Design 3 using silver-based nanofluid. These results underscored the potential of CuO nanoparticle-based nanofluids in battery thermal management systems.

Overall, the above findings have demonstrated that Ag nanofluids, particularly when employed in Design 3 with its serpentine flow pattern, offer significant improvements in cooling performance compared to water cooling and CuO nanofluids. This highlights the importance of not only the nanofluid properties but also the adoption of innovative mini-channel design for effective battery thermal management.

Funding

No funding was received for this work.

Data availability statement

The data underlying this article will be shared on reasonable request to the corresponding authors.

Conflict of interest

The authors declare no conflict of interest.

References

[1] A.M. Abdalla, et al., Innovative lithium-ion battery recycling: sustainable process for recovery of critical materials from lithium-ion batteries, J. Energy Storage 67 (Sep. 2023) 107551, https://doi.org/10.1016/j.est.2023.107551.
[2] A. Dhanasekaran, et al., Thermal Management of Pouch-type Li-ion Batteries: A Computational Analysis, 2024, p. 020029., https://doi.org/10.1063/5.0225542.
[3] Y. Subramanian, et al., A review on applications of carbon nanotubes-based metal-sulfide composite anode materials (CNTs/MS) for sodium (Na)-ion batteries, Emergent Mater. (May 2023), https://doi.org/10.1007/s42247-023-00501-3.
[4] T. Wang, et al., Performance of plug-in hybrid electric vehicle under low temperature condition and economy analysis of battery pre-heating, J. Power Sources 401 (Oct. 2018) 245–254, https://doi.org/10.1016/j.jpowsour.2018.08.093.
[5] S.L. Vendra, G. Singh, R. Kumar, Single source precursor-derived SiOC/TiOxCy as an anode component for Li-ion batteries, Int. J. Appl. Ceram. Technol. 20 (1) (Jan. 2023) 70–83, https://doi.org/10.1111/ijac.14237.
[6] F.H. Gandoman, et al., Concept of reliability and safety assessment of lithium-ion batteries in electric vehicles: basics, progress, and challenges, Appl. Energy 251 (Oct. 2019) 113343, https://doi.org/10.1016/j.apenergy.2019.113343.
[7] B.Y. Liaw, E.P. Roth, R.G. Jungst, G. Nagasubramanian, H.L. Case, D.H. Doughty, Correlation of Arrhenius behaviors in power and capacity fades with cell impedance and heat generation in cylindrical lithium-ion cells, J. Power Sources 119 (121) (Jun. 2003) 874–886, https://doi.org/10.1016/S0378-7753(03)00196-4.
[8] M. Ouyang, et al., Low temperature aging mechanism identification and lithium deposition in a large format lithium iron phosphate battery for different charge profiles, J. Power Sources 286 (Jul. 2015) 309–320, https://doi.org/10.1016/j.jpowsour.2015.03.178.
[9] A.A. Pesaran, Battery thermal models for hybrid vehicle simulations, J. Power Sources 110 (2) (Aug. 2002) 377–382, https://doi.org/10.1016/S0378-7753(02)00200-8.
[10] H. Fan, L. Wang, W. Chen, B. Liu, P. Wang, A J-type air-cooled battery thermal management system design and optimization based on the electro-thermal coupled model, Energies 16 (16) (Aug. 2023) 5962, https://doi.org/10.3390/en16165962.
[11] M. Wang, T.-C. Hung, H. Xi, Numerical study on performance enhancement of the air-cooled battery thermal management system by adding parallel plates, Energies 14 (11) (May 2021) 3096, https://doi.org/10.3390/en14113096.
[12] J. Xu, Z. Guo, Z. Xu, X. Zhou, X. Mei, A systematic review and comparison of liquid-based cooling system for lithium-ion batteries, eTransportation 17 (Jul. 2023) 100242, https://doi.org/10.1016/j.etran.2023.100242.
[13] N. Mei, X. Xu, R. Li, Heat dissipation analysis on the liquid cooling system coupled with a flat heat pipe of a lithium-ion battery, ACS Omega. 5 (28) (Jul. 2020) 17431–17441, https://doi.org/10.1021/acsomega.0c01858.
[14] A.R. Bais, D.G. Subhedhar, N.C. Joshi, S. Panchal, Numerical investigation on thermal management system for lithium ion battery using phase change material, Mater. Today Proc. 66 (2022) 1726–1733, https://doi.org/10.1016/j.matpr.2022.05.269.
[15] L. Ianniciello, P.H. Biwolé, P. Achard, Electric vehicles batteries thermal management systems employing phase change materials, J. Power Sources 378 (Feb. 2018) 383–403, https://doi.org/10.1016/j.jpowsour.2017.12.071.
[16] R. Zhou, Y. Chen, J. Zhang, P. Guo, Research progress in liquid cooling technologies to enhance the thermal management of LIBs, Mater. Adv. 4 (18) (2023) 4011–4040, https://doi.org/10.1039/D3MA00299C.
[17] Y. Huo, Z. Rao, X. Liu, J. Zhao, Investigation of power battery thermal management by using mini-channel cold plate, Energy Convers. Manag. 89 (Jan. 2015) 387–395, https://doi.org/10.1016/j.enconman.2014.10.015.
[18] Z. An, K. Shah, L. Jia, Y. Ma, A parametric study for optimization of minichannel based battery thermal management system, Appl. Therm. Eng. 154 (May 2019) 593–601, https://doi.org/10.1016/j.applthermaleng.2019.02.088.
[19] N. Wu, X. Li, N. Ouyang, W. Zhang, Mini-channel liquid cooling system for large-sized lithium-ion battery packs by integrating step-allocated coolant scheme, Appl. Therm. Eng. 214 (Sep. 2022) 118798, https://doi.org/10.1016/j.applthermaleng.2022.118798.
[20] L.W. Jin, P.S. Lee, X.X. Kong, Y. Fan, S.K. Chou, Ultra-thin minichannel LCP for EV battery thermal management, Appl. Energy 113 (Jan. 2014) 1786–1794, https://doi.org/10.1016/j.apenergy.2013.07.013.
[21] T. Deng, G. Zhang, Y. Ran, Study on thermal management of rectangular Li-ion battery with serpentine-channel cold plate, Int. J. Heat Mass Tran. 125 (Oct. 2018) 143–152, https://doi.org/10.1016/j.ijheatmasstransfer.2018.04.065.
[22] A. Jarrett, I.Y. Kim, Design optimization of electric vehicle battery cooling plates for thermal performance, J. Power Sources 196 (23) (Dec. 2011) 10359–10368, https://doi.org/10.1016/j.jpowsour.2011.06.090.
[23] S.M.S. Murshed, K.C. Leong, C. Yang, Investigations of thermal conductivity and viscosity of nanofluids, Int. J. Therm. Sci. 47 (5) (May 2008) 560–568, https://doi.org/10.1016/j.ijthermalsci.2007.05.004.
[24] W.H. Azmi, K.V. Sharma, R. Mamat, G. Najafi, M.S. Mohamad, The enhancement of effective thermal conductivity and effective dynamic viscosity of nanofluids – a review, Renew. Sustain. Energy Rev. 53 (Jan. 2016) 1046–1058, https://doi.org/10.1016/j.rser.2015.09.081.
[25] A. Dhanasekaran, et al., Silver nanofluid-based thermal management for effective cooling of batteries in electric vehicle systems, Arabian J. Sci. Eng. (Feb. 2024), https://doi.org/10.1007/s13369-024-08790-4.
[26] M.A. Abdelkareem, et al., Battery thermal management systems based on nanofluids for electric vehicles, J. Energy Storage 50 (Jun. 2022) 104385, https://doi.org/10.1016/j.est.2022.104385.
[27] H. Liu, E. Chika, J. Zhao, Investigation into the effectiveness of nanofluids on the mini-channel thermal management for high power lithium ion battery, Appl. Therm. Eng. 142 (Sep. 2018) 511–523, https://doi.org/10.1016/j.applthermaleng.2018.07.037.
[28] L.R. Rosa, R.D. Rosa, M.A.M.S. da Veiga, Colloidal silver and silver nanoparticles bioaccessibility in drinking water filters, J. Environ. Chem. Eng. 4 (3) (Sep. 2016) 3451–3458, https://doi.org/10.1016/j.jece.2016.07.017.
[29] B. Buszewski, K. Rafiłska, P. Pomastowski, J. Walczak, A. Rogowska, Novel aspects of silver nanoparticles functionalization, Colloids Surfaces A Physicochem. Eng. Asp. 506 (Oct. 2016) 170–178, https://doi.org/10.1016/j.colsurfa.2016.05.058.
[30] S. Du, et al., Study on the thermal behaviors of power lithium iron phosphate (LFP) aluminum-laminated battery with different tab configurations, Int. J. Therm. Sci. 89 (Mar. 2015) 327–336, https://doi.org/10.1016/j.ijthermalsci.2014.11.018.

[31] C. Zhao, A.C.M. Sousa, F. Jiang, Minimization of thermal non-uniformity in lithium-ion battery pack cooled by channeled liquid flow, Int. J. Heat Mass Tran. 129 (Feb. 2019) 660—670, https://doi.org/10.1016/j.ijheatmasstransfer.2018.10.017.
[32] O. Yetik, N. Yilmaz, T.H. Karakoc, Computational modeling of a <scp>lithium-ion</scp> battery thermal management system with <scp> Al_2 O_3 -based </scp> nanofluids, Int. J. Energy Res. 45 (9) (Jul. 2021) 13851—13864, https://doi.org/10.1002/er.6718.
[33] H. Li, X. Xiao, Y. Wang, C. Lian, Q. Li, Z. Wang, Performance investigation of a battery thermal management system with microencapsulated phase change material suspension, Appl. Therm. Eng. 180 (Nov. 2020) 115795, https://doi.org/10.1016/j.applthermaleng.2020.115795.
[34] S. Wiriyasart, C. Hommalee, S. Sirikasemsuk, R. Prurapark, P. Naphon, "Thermal management system with nanofluids for electric vehicle battery cooling modules," Case Stud. Therm. Eng. 18 (Apr. 2020) 100583, https://doi.org/10.1016/j.csite.2020.100583.
[35] F.M. Nasir, M.Z. Abdullah, M.F.M.A. Majid, M.A. Ismail, Nanofluid-filled heat pipes in managing the temperature of EV lithium-ion batteries, J. Phys. Conf. Ser. 1349 (1) (Nov. 2019) 012123, https://doi.org/10.1088/1742-6596/1349/1/012123.
[36] A.M. Hussein, R.A. Bakar, K. Kadirgama, K.V. Sharma, Experimental measurements of nanofluids thermal properties, Int. J. Automot. Mech. Eng. 7 (Jun. 2013) 850—863, https://doi.org/10.15282/ijame.7.2012.5.0070.
[37] Qamar Fairuz Zahmani, Norzelawati Asmuin, Mohamad Kamil Sued, Siti Nor'ain Mokhtar, Muhammad Nazrul Hakimi Sahar, Nanofluid-infused microchannel heat sinks: comparative study of Al2O3, TiO2, and CuO to optimized thermal efficiency, J. Adv. Res. Micro Nano Engieering 19 (1) (May 2024) 1—12, https://doi.org/10.37934/armne.19.1.112.
[38] M. Patil, S. Panchal, N. Kim, M.-Y. Lee, Cooling performance characteristics of 20 Ah lithium-ion pouch cell with cold plates along both surfaces, Energies 11 (10) (Sep. 2018) 2550, https://doi.org/10.3390/en11102550.
[39] M.B. Nejad, H.A. Mohammed, O. Sadeghi, S.A. Zubeer, Influence of nanofluids on the efficiency of flat-plate solar collectors (FPSC), E3S Web Conf. 22 (Nov. 2017) 00123, https://doi.org/10.1051/e3sconf/20172200123.
[40] S.H. Pourhoseini, N. Naghizadeh, H. Hoseinzadeh, Effect of silver-water nanofluid on heat transfer performance of a plate heat exchanger: an experimental and theoretical study, Powder Technol. 332 (Jun. 2018) 279—286, https://doi.org/10.1016/j.powtec.2018.03.058.
[41] L. Godson, K. Deepak, C. Enoch, B. Jefferson, B. Raja, Heat transfer characteristics of silver/water nanofluids in a shell and tube heat exchanger, Arch. Civ. Mech. Eng. 14 (3) (May 2014) 489—496, https://doi.org/10.1016/j.acme.2013.08.002.
[42] B. Adebayo-Tayo, A. Salaam, A. Ajibade, Green synthesis of silver nanoparticle using Oscillatoria sp. extract, its antibacterial, antibiofilm potential and cytotoxicity activity, Heliyon 5 (10) (Oct. 2019) e02502, https://doi.org/10.1016/j.heliyon.2019.e02502.
[43] L. Sheng, et al., Numerical investigation on a lithium ion battery thermal management utilizing a serpentine-channel liquid cooling plate exchanger, Int. J. Heat Mass Tran. 141 (Oct. 2019) 658—668, https://doi.org/10.1016/j.ijheatmasstransfer.2019.07.033.
[44] S. Lin, L. Zhou, Thermal performance of rectangular serpentine mini-channel cooling system on lithium battery, J. Clean. Prod. 418 (Sep. 2023) 138125, https://doi.org/10.1016/j.jclepro.2023.138125.
[45] A. Ozsoy, V. Corumlu, Thermal performance of a thermosyphon heat pipe evacuated tube solar collector using silver-water nanofluid for commercial applications, Renew. Energy 122 (Jul. 2018) 26—34, https://doi.org/10.1016/j.renene.2018.01.031.
[46] S. Iyahraja, J.S. Rajadurai, Stability of aqueous nanofluids containing PVP-coated silver nanoparticles, Arabian J. Sci. Eng. 41 (2) (Feb. 2016) 653—660, https://doi.org/10.1007/s13369-015-1707-9.
[47] S. Ye, A.R. Rathmell, Y. Ha, A.R. Wilson, B.J. Wiley, The role of cuprous oxide seeds in the one-pot and seeded syntheses of copper nanowires, Small 10 (9) (May 2014) 1771—1778, https://doi.org/10.1002/smll.201303005.
[48] N.O.H. Tani, Production of Copper Powder, US Pat, 1998 5850047.